Published OnlineFirst November 4, 2016; DOI: 10.1158/1078-0432.CCR-16-1524

Cancer Therapy: Preclinical

Clinical Cancer Research

Cytokine-Induced Killer Cells Kill Chemo-surviving Melanoma Cancer Stem Cells

Loretta Gammaitoni[1], Lidia Giraudo[1], Marco Macagno[1,2], Valeria Leuci[1,2], Giulia Mesiano[1], Ramona Rotolo[1,2], Francesco Sassi[3], Martina Sanlorenzo[1,2,4], Alessandro Zaccagna[5], Alberto Pisacane[6], Rebecca Senetta[6], Michela Cangemi[2], Giulia Cattaneo[1,2], Valentina Martin[1], Valentina Coha[1], Susanna Gallo[1], Ymera Pignochino[1,3], Anna Sapino[6], Giovanni Grignani[1], Fabrizio Carnevale-Schianca[1], Massimo Aglietta[1,2], and Dario Sangiolo[1,2]

Abstract

Purpose: The MHC-unrestricted activity of cytokine-induced killer (CIK) cells against chemo-surviving melanoma cancer stem cells (mCSC) was explored, as CSCs are considered responsible for chemoresistance and relapses.

Experimental Design: Putative mCSCs were visualized by engineering patient-derived melanoma cells (MC) with a lentiviral vector encoding eGFP under expression control by stemness gene promoter *oct4*. Their stemness potential was confirmed *in vivo* by limiting dilution assays. We explored the sensitivity of eGFP$^+$ mCSCs to chemotherapy (CHT), BRAF inhibitor (BRAFi) or CIK cells, as single agents or in sequence, *in vitro*. First, we treated MCs *in vitro* with fotemustine or dabrafenib (BRAF-mutated cases); then, surviving MCs, enriched in mCSCs, were challenged with autologous CIK cells. CIK cell activity against chemoresistant mCSCs was confirmed *in vivo* in two distinct immunodeficient murine models.

Results: We visualized eGFP$^+$ mCSCs (14% $\pm$ 2.1%) in 11 MCs. The tumorigenic precursor rate *in vivo* was higher within eGFP$^+$ MCs (1/42) compared with the eGFP$^-$ counterpart (1/4,870). *In vitro* mCSCs were relatively resistant to CHT and BRAFi, but killed by CIK cells ($n = 11$, 8/11 autologous), with specific lysis ranging from 95% [effector:tumor ratio (E:T), 40:1] to 20% (E:T 1:3). *In vivo* infusion of autologous CIK cells into mice bearing xenografts from three distinct melanomas demonstrated significant tumor responses involving CHT-spared eGFP$^+$ mCSCs ($P = 0.001$). Sequential CHT–immunotherapy treatment retained antitumor activity ($n = 12$, $P = 0.001$) reducing mCSC rates ($P = 0.01$).

Conclusions: These findings are the first demonstration that immunotherapy with CIK cells is active against autologous mCSCs surviving CHT or BRAFi. An experimental platform for mCSC study and rationale for CIK cells in melanoma clinical study is provided. *Clin Cancer Res; 23(9); 2277–88. ©2016 AACR.*

Introduction

Malignant melanoma is the most aggressive form of skin cancer. While localized tumors are curable with surgery, treatment possibilities for metastatic melanoma have long been limited due to its minimal response to conventional anticancer treatments (1). Recently, molecular targeted therapy and immunotherapy have greatly advanced metastatic melanoma treatment by employing, respectively, small molecules inhibiting mutated forms of *b-raf* (2–4) and immune checkpoint inhibitors ipilimumab (5), nivolumab (6, 7), and pembrolizumab (8) to achieve such remarkable clinical trial results that they are now first-line options in international treatment guidelines (9–11). Despite these treatments, a consistent portion of patients relapse or does not achieve disease control. In addition to checkpoint inhibitors, adoptive immunotherapy also appears highly promising, and after decades of preclinical relegation, is starting to find its way into clinical applications (12, 13). While the two approaches may be complementary, tumors containing relatively few immunogenic mutations, or those with a "noninflamed" tumor microenvironment, continue to represent an important immunotherapy challenge. Specifically, in some nonresponsive or relapsing patient subsets, or when attempting to hit tumor-sustaining targets like cancer stem cells (CSC), adoptive infusion of *ex vivo* expanded antitumor immune effectors is worth consideration.

Crucial to new therapeutic strategy planning is CSC analysis and targeting because this cell subpopulation is a key factor in chemotherapeutic agent and radiotherapy resistances, contributes to posttreatment relapse, and is involved in tumor metastasis (14–21). The fact that conventional chemotherapies preferentially target actively- cycling cells, as opposed to CSCs, may implicate

[1]Division of Medical Oncology, Experimental Cell Therapy, Candiolo Cancer Institute, FPO-IRCCS, Candiolo, Torino, Italy. [2]Department of Oncology, University of Torino, Candiolo, Torino, Italy. [3]Laboratory of Translational Cancer Medicine, Candiolo Cancer Institute, FPO-IRCCS, Candiolo, Torino, Italy. [4]Section of Dermatology, Department of Medical Sciences, University of Torino, Torino, Italy. [5]Surgical Dermatology, Candiolo Cancer Institute, FPO-IRCCS, Candiolo, Torino, Italy. [6]Pathology, Candiolo Cancer Institute, FPO-IRCCS, Candiolo, Torino, Italy.

Note: Supplementary data for this article are available at Clinical Cancer Research Online (http://clincancerres.aacrjournals.org/).

Corresponding Author: Dario Sangiolo, Department of Oncology, University of Torino, Candiolo Cancer Institute IRCCs, Candiolo, 10060, Italy. Phone: 3901-1993-3521; Fax: 3901-1993-3522; E-mail: dario.sangiolo@unito.it

doi: 10.1158/1078-0432.CCR-16-1524

Published OnlineFirst November 4, 2016; DOI: 10.1158/1078-0432.CCR-16-1524

Translational Relevance

This work reports the effective antitumor activity of patient-derived cytokine-induced killer (CIK) cells against autologous chemoresistant melanoma cancer stem cells (CSC). CSCs are clinically relevant targets, associated with disease relapse. We demonstrate that CHT kills proliferating melanoma cells but spares tumorigenic CSCs, *in vitro* and *in vivo*. The MHC-independent immunotherapy with CIK cells proved successful in this challenging framework. Consistent findings were obtained in selected cases of *braf*-mutated melanoma treated with small-molecule BRAFi. Our data, generated within an autologous system, support the exploration of CIK cells in clinical trials. Cost effectiveness, safety profile, and the ability to overcome tumor MHC downregulation are favorable issues to be considered in clinical perspective. CIK cells may be integrated at different levels in the composite therapeutic scenario of metastatic melanoma, offering an additional weapon to control tumor spread and promote its eradication.

these observed treatment failures. Thus, exploration of novel therapeutic strategies to target CSCs with immunotherapy holds great potential (21–27).

Among the various adoptive immunotherapy approaches, we focused on an MHC-independent strategy based on cytokine-induced killer (CIK) cells (28–32), which are *ex vivo*–expanded T-NK lymphocytes with MHC-independent antitumor activity (33–38). The principal mechanism of tumor killing is recognition of stress-inducible tumor-restricted molecules (e.g., MIC A/B; ULBPs 1–6) by the NKG2D receptor (35, 36, 39). Preclinical studies of intense CIK cell activity against several tumors have been reported, as has recent evidence of their successful redirection with chimeric–antigen receptors (CAR; refs. 40–42). Moreover, initial clinical trials demonstrated their safety profile, supporting their potential against solid tumors (37, 38, 43, 44).

We previously reported preclinical CIK cell activity against autologous melanoma and initial *in vitro* data against putative mCSCs (31). MHC-independent immunotherapeutic approaches may present advantages over antigen-specific adaptive immune responses against CSCs. Indeed, effectors like CIK cells, or even natural killer and γδ T cells, are unaffected by tumor-defensive downregulation of HLA molecules, and their activating targets (e.g., MIC A/B; ULBPs) are associated and expressed in undifferentiated tumor cells (22, 31, 32, 45–47).

This investigation builds on our previous findings. It explores the preclinical activity of CIK cells against autologous melanoma, focusing on mCSCs that may survive conventional chemo- or molecular targeted therapies. To visualize putative CSCs, we used a strategy previously validated in our laboratory that relies on a lentiviral vector encoding the enhanced GFP (eGFP) under expression control of the human *oct4* promoter (LV. Oct4.eGFP). The underlying idea is to reveal CSCs exploiting their selective ability to activate a well-characterized stemness promoter (31, 32, 48). Our central hypothesis is that chemotherapy (CHT) kills proliferating tumor cells, and thereby reduces the tumor burden, but spares CSCs that support disease relapse. We simulated this scenario in an autologous preclinical model, both *in vitro* and *in vivo*, and then assessed the efficacy of immunotherapy with CIK cells.

Materials and Methods

Establishment of patient-derived melanoma cell cultures

Human melanoma tissues were obtained from 11 surgical specimens (lymphnodal or cutaneous metastasis); patients with advanced stage melanoma provided consent under Institutional Review Board–approved protocols. Human melanoma tissues were cut into 3-mm^3 pieces and processed for cell isolation. Tumor tissue was processed and melanoma cells were cultured as described previously (31).

Characterization of patient-derived melanoma cell cultures

Cell aliquots from patient-derived melanoma cell cultures were stained with FITC, PE, PE-Cyanin 7 (PC7), or APC-conjugated mouse mAbs against extracellular and intracytoplasmic human antigens [anti-CD271-PE, anti-OCT3/4-PE, anti-SOX2-APC, and anti-NANOG-PerCP-Cy5.5 (BD Biosciences Italy, Pharmingen); anti-MCSP-APC (Miltenyi Biotec Srl), anti-VEGFR1-APC and anti-ABCG2-PE (R&D Systems, Space Import Export); anti-MITF (Abcam, Prodotti Gianni Srl)], anti-HLA-ABC-FITC and anti-PD-L1-PE (BD Biosciences, Pharmingen); CIK-target antigens [anti-MIC A/B (BD Biosciences, Pharmingen); anti-ULBPs, anti-CD112, and anti-CD155 (R&D System, Space Import Export, Milan, Italy)]. Intracellular expression of OCT4 and MITF was detected after fixation/permeabilization by the Cytoperm/Cytofix kit per manufacturer's instructions (BD Biosciences, Pharmingen). To detect MITF, we used a secondary goat antimouse PE-labeled mAb (Abcam, Prodotti Gianni Srl). Labeled cells were read on FACS Cyan (CyAn ADP, Beckman Coulter s.r.l.) and analyzed using Summit Software. Gate criteria were set to isotype controls.

CIK culture, expansion, and characterization

Human peripheral blood samples were obtained from subjects with histologically confirmed advanced stage melanoma at the Candiolo Cancer Institute, Fondazione del Piemonte per l'Oncologia (FPO)–IRCCS (Candiolo, Torino, Italy). All individuals provided their informed consent.

Cultures were started with peripheral blood mononuclear cells (PBMC) collected from 8 of 11 metastatic melanoma (mMel) patients, surgically treated and performed as described previously (31, 32). Briefly, PBMCs isolated by density gradient (Lymphosep, Aurogene s.r.l.) and centrifugation were cultured at a cell density of 1.5×10^6 cells/mL in RPMI (Gibco BRL Life Technologies), supplemented with 10% FBS (Sigma), and with timed additions of 1,000 U/mL IFNγ at day 0 (Miltenyi Biotec Srl), 50 ng/mL anti-CD3 antibody at day +1 (Miltenyi Biotec Srl), and 300 U/mL recombinant human IL2 (from day +1, refreshed every 3–4 days until the end of the expansion; Miltenyi Biotec Srl).

Phenotypic analysis of CIK cells was performed weekly, using the following fluorescein isothiocyanate (FITC), phycoerythrin (PE), or allophycocyanin (APC)-conjugated mouse mAbs: CD3-FITC, CD8-PE, CD56-APC, and CD314-APC (aka anti-NKG2D; mAbs; all from Miltenyi Biotec Srl) and anti-DNAM-1 (BD Biosciences Italy, Pharmingen).

Labeled cells were read on FACS Cyan (CyAn ADP, Beckman Coulter s.r.l.) and analyzed using Summit Software. Gate criteria were set to isotype controls.

Published OnlineFirst November 4, 2016; DOI: 10.1158/1078-0432.CCR-16-1524

hOct4.eGFP lentiviral vector generation

VSV-G pseudotyped third-generation lentiviral vectors (LV) were produced by transient four-plasmid cotransfection into 293T cells (49, 50). Transfer vector pRRL.sin.PPT.hPGK.EGFP.Wpre (LV.PGK.EGFP), kindly provided by Dr. Elisa Vigna (Gene Transfer and Therapy, IRCCS Candiolo, Turin, Italy), has been described elsewhere.

The phOCT4.EGFP1 vector (48) was kindly provided by Dr. Wei Cui (IRDB, Imperial College, London, United Kingdom). The pRRL.sin.PPT.hOct4.eGFP.Wpre (LV-Oct4.eGFP) was obtained by replacing expression cassette hPGK.eGFP in LV-PGK.eGFP with hOct4-eGFP1 cleaved from the phOct4-eGFP1 vector through insertion into the *Sal*I and *Xho*I restriction enzyme sites. Physical titers for lentiviral vector stocks were determined on the basis of p24 antigen content (HIV-1 p24 ELISA kit; PerkinElmer).

Patient-derived melanoma cell transduction

For each LV transduction, patient-derived melanoma cells were cultured in fresh KODMEM-F12 with 10% FBS. Virus-conditioned medium was added at a dose of 400 ng P24/1 $\times$ 10^5 cells. After 16 hours, cells were washed twice and grown for a minimum of 10 days to reach steady-state eGFP expression and to rule out pseudo-transduction prior to flow cytometry analysis (31). As a transduction efficiency control, the same melanoma primary cells were transduced with LV.PGK.eGFP.

In vitro assessment of CSC sensitivity to fotemustine or dabrafenib

LV.Oct4.eGFP–transduced melanoma cells were seeded into 6-well plates (12–18 $\times$ 10^4 cells/well). After overnight incubation, cells were treated with the half-maximal inhibitory concentration (IC_{50}) dose of fotemustine (Muphoran ItalFarmaco) or dabrafenib (BRAFi GSK2118436, Sequoia Research Products) for 72 hours. LV.Oct4.eGFP–transduced melanoma cells treated with an equal volume of drug diluent were utilized as the control. At the end of treatment, cells were harvested and counted. The cell viability was determined with Trypan Blue 0.1% exclusion dye and an automated cell counter Countess (Invitrogen) according to the manufacturer's instructions. The percentage of $eGFP^+$ cells was determined by flow cytometry (CyAn ADP, Beckman Coulter s.r.l.). The eGFP positivity was calculated on viable cell fraction, detected by 4′,6-diamidino-2-phenylindole (DAPI) permeability exclusion assay. Treatment effects were measured by conducting four to six independent experiments, each of which included six replicates. The eGFP increment, expressed as fold increase, was separately calculated for each experiment to compare fotemustine- or BRAFi-treated samples with their internal untreated control.

In vitro cytotoxicity assay with CIK cells against melanoma

CIK tumor-killing ability was assessed against 11 LV.Oct4.eGFP–transduced patient-derived melanoma cells. Effector cells were assayed against autologous tumor targets when possible (8/11). In the absence of autologous PBMCs (3/11), CIK cells were generated from other melanoma patients and employed as allogenic effectors. All melanoma cell cultures were assayed with allogeneic CIK cells as controls. Their immune-mediated killing was analyzed assessing target cell viability by flow cytometry (CyAn ADP Beckman Coulter s.r.l.) by DAPI permeability. CIK cells were cocultured with targets (either autologous or allogenic LV.Oct4.eGFP–transduced melanoma cells) previously treated for 72 hours with fotemustine or dabrafenib (IC_{50} dose) or an equal diluent volume as a control. Essays were conducted at progressively decreasing effector:target (E:T) ratios, 40:1, 20:1, 10:1, 5:1, 3:1, 1:1, 2:1, and 1:3 for 72 hours in 200 μL of medium with IL2 at a concentration of 300 U/mL at 37°C 5% CO_2. A confirmatory method was tested in parallel to determine the number of viable, metabolically active, target cells in culture, based on the quantitation of ATP present (CellTiter-Glo Luminescent Cell Viability Assay, Promega Italia s.r.l).

Tumor cells, in the absence of CIK cells, were used as a control to assess spontaneous mortality. The percentage of tumor-specific lysis for each E:T ratio was calculated as experimental−spontaneous mortality/100−spontaneous mortality) $\times$ 100. The curve also allowed us to calculate the IC_{50} value for each melanoma culture.

In vivo activity assay against mCSCs

Six-week-old NOD/LtSz-scid/scid (NOD/SCID; Charles River Laboratories) female mice were subcutaneously injected with 5 $\times$ 10^5 LVs. Oct4.eGFP–transduced patient-derived melanoma cells (mMel7 $n = 34$, mMel11 $n = 40$) were cultured in equal volumes of sterile PBS1$\times$ and BD Matrigel Basement Membrane Matrix (BD Biosciences Italy). Treatments started when tumors became palpable. Mice from CIK immunotherapy group (mMel7, $n = 10$; mMel11, $n = 12$) received 4 intravenous infusions (1 $\times$ 10^7 mouse every 3–4 days) of mature CIK cells (resuspended in 200 μL of 1$\times$ PBS) without systemic administration of IL2. Mice from CHT group ($n = 34$) received two intraperitoneal injections of fotemustine (600 μg/mouse days 1;15), while mice injected with PBS alone ($n = 18$) represented untreated controls.

An early part of the experiment (group A: CIK-immunotherapy $n = 10$, CHT $n = 10$, PBS $n = 8$) was terminated and analyzed after 2 weeks (day +15) to assess the antitumor activity (Ki67 proliferative index) and residual rate of $eGFP^+$ mCSCs. A second branch (group B) of the experiment proceeded beyond day +15 to explore the effect of chemo-immunotherapy combination. Mice ($n = 12$) from the initial CHT cohort (treated with fotemustine on days 1;15) started intravenous infusions with CIK cells (1 $\times$ 10^7/mouse every 4–5 days from a minimum of 2 weeks to a maximum of 10 weeks); remaining mice from all the initial cohorts (CIK-immunotherapy, $n = 12$; CHT, $n = 12$; PBS, $n = 10$) worked as control and continued to be infused with PBS alone up to the end of the experiment. In all cases, the experiment was terminated and animals euthanized when tumor size reached 2 cm in its main diameter, unacceptable toxicity occurred, or CIK cell infusions ended, whichever occurred first.

Tumor growth was monitored weekly with calipers and volume calculated according to the formula: $V = 4/3 \times \pi \times (l/2)^2 \times (L/2)$, where L is the length and l the width diameter of the tumor. The recovered tumors were aliquoted. A first aliquot was fixed overnight in 4% paraformaldehyde, then dehydrated, paraffin-embedded, and sectioned (5 μm) and finally stained with hematoxylin and eosin (H&E) (Bio Optica). To assess the antitumor activity, tumor sections were stained for immunohistochemistry assay with Ki67 antibody (Dako-Agilent Technologies Italia S.p.A; ref. 32). To assess CIK cell infiltrate, immunohistochemical assay was performed with human anti-CD3 antibodies (Novocastra, Leica Biosystems) and assessed by a pathologist. A second aliquot was processed by mechanical

Published OnlineFirst November 4, 2016; DOI: 10.1158/1078-0432.CCR-16-1524

and enzymatic dissociation using the Tumor Dissociation kit, human and the gentleMACS dissociator, according to the manufacturer's instructions (Miltenyi Biotec S.r.l.). Monocellular suspensions obtained after dissociation were filtered using 70-μm CellStrainer and the percentage of eGFP$^+$ cells was determined by flow cytometry (CyAn ADP, Beckman Coulter s.r.l.) and analyzed using Summit Software.

Patient-derived xenografts

Six-week-old NOD/SCID (Charles River Laboratories) female mice were subcutaneously injected with an 8 mm^3 tumor fragment from patient-derived melanoma biopsies (mMel2 and mMel3). Starting one week after tumor implantation, mice ($n = 14$) received 8 weekly intravenous infusions of 1×10^7 mature autologous CIK cells in 1× PBS (200-μL total volume injected) without systemic administration of IL2. Mice ($n = 13$) injected with PBS alone were used as the untreated control. Tumor growth was monitored weekly as described above. Animals were euthanized at experiment end or when tumor size reached 2 cm in its main diameter. The recovered tumors were fixed overnight in 4% paraformaldehyde, dehydrated, paraffin-embedded, sectioned (5 μm), and finally stained for immunohistochemical assay with Ki67 antibody (Dako Italia Spa). In a selected experiment, the recovered tumors were mechanically and subsequently enzymatically dissociated (Collagenase Type I, Invitrogen) for 3 hours. Monocellular suspensions obtained after dissociation were filtered using 70-μm CellStrainer (Becton Dickinson BD Biosciences Italy) and LV.Oct4.eGFP transduced as described previously. The percentage of eGFP$^+$ cells was determined by flow cytometry (CyAn ADP Beckman Coulter s.r.l.) 3 days after transduction and analyzed using Summit Software.

Statistical analysis

Statistical analysis was performed using software GraphPad Prism 6. A descriptive statistical analysis of CIK and melanoma cell median or mean values was used as appropriate. The relative increase of eGFP$^+$ mCSC in melanoma samples, treated either *in vitro* or *in vivo* with fotemustine, BRAFi, or CIK cells, were compared with controls by unpaired *t* test. Comparison of Ki67 proliferative index between melanoma samples, treated *in vivo* with either fotemustine or CIK cells, were compared with controls by unpaired *t* test.

The mixed-model ANOVA was employed to assess CIK cytotoxic activity curves *in vitro*. Statistical significance has been expressed as *P* value, and all values less than 0.05 were considered statistically significant. The CSC frequency was calculated with L-Calc T software program (Stem Cell Technologies Company, Voden Medical Instruments S.p.a), which uses Poisson statistics and the method of maximum likelihood.

Results

Putative mCSCs survive CHT *in vitro*

Melanoma cell cultures and visualization of putative mCSCs. We established 11 melanoma cell cultures from metastatic tissue biopsied from 11 patients with advanced stage melanoma (Supplementary Table S1). *Braf* mutational analysis revealed that 5 of 11 of the patient-derived cell cultures were *braf*-mutated (4 V600E: mMel3, mMel7, mMel11, mMel15, 1 V600K: mMel2).

Each culture was assessed for expression of the main melanoma surface antigens: melanoma-associated chondroitin sulfate proteoglycan (MCSP), nervous growth factor receptor (NGFR, a.k.a CD271), and VEGFR1 (Table 1). All tumors retained membrane expression of HLA class I molecules (>99% HLA-ABC$^+$; data not shown).

We visualized putative mCSCs by a gene transfer strategy (27, 28) based on the stable transduction of patient-derived melanoma cells with a lentiviral vector encoding eGFP under the control of the *oct4* gene promoter regulatory element (LV. Oct4.eGFP; Supplementary Fig. S1A–S1D; Supplementary Table S2). Using this approach, the average rate of eGFP$^+$ mCSC within the 11 cultures was 12% ± 2.1% (Table 1). As parallel control, we confirmed that melanoma cells could be transduced efficiently (>95%) when the strong ubiquitous promoter (Phospho Glycerato Kinase, PGK, regulatory element) was utilized in place of the *oct4* promoter to control eGFP expression (Supplementary Fig. S1E and S1F; Supplementary Table S2). Furthermore, the integration of LV.Oct4. eGFP was confirmed by PCR in both eGFP$^+$ and eGFP$^-$ melanoma cell subsets (Supplementary Fig. S1G).

Each melanoma culture was assessed for expression of the principal ligands recognized by CIK cell receptors NKG2D (MIC A/B, ULBP1, ULBP2-5-6, and ULBP3) and DNAM-1 (CD112 and CD155). As Table 1 indicates, MIC A/B and ULBP2-5-6 were expressed in all melanomas. Although sample values generally varied highly, MIC A/B and ULBP2-5-6 were comparable in eGFP$^+$mCSC and eGFP$^-$ melanoma cells (Fig. 1A and B). The expression of ULBP1, ULBP 3, CD112, and CD155 was negligible

Table 1. Immunophenotype of melanoma cell cultures

n. Melanoma	eGFP[a,b]	MCSP[a]	MIC A/B[a]	ULBP2,5,6[a]	NGFR[a]	VEGFR1[a]	PD-L1[a]
mMel1	21	65	34	63	74	89	2
mMel2	8	71	15	41	58	95	0
mMel3	2	81	90	98	93	98	0
mMel7	17	78	21	65	39	89	2
mMel11	24	95	2	44	67	94	0
mMel12	16	94	86	60	14	89	6
mMel13	14	80	2	40	9	95	9
mMel14	13	79	10	59	93	95	2
mMel15	4	92	2	58	58	97	1
mMel16	11	33	6	52	10	85	6
mMel17	5	70	0	15	52	58	2
Average	12	76	24	54	52	89	3
SEM	2	5	10	6	9	3	1

[a]Value expressed as percentage of viable positive cells.
[b]eGFP analyzed on viable cells ≥10 days after transduction with LV.Oct4.eGFP vector.

Published OnlineFirst November 4, 2016; DOI: 10.1158/1078-0432.CCR-16-1524

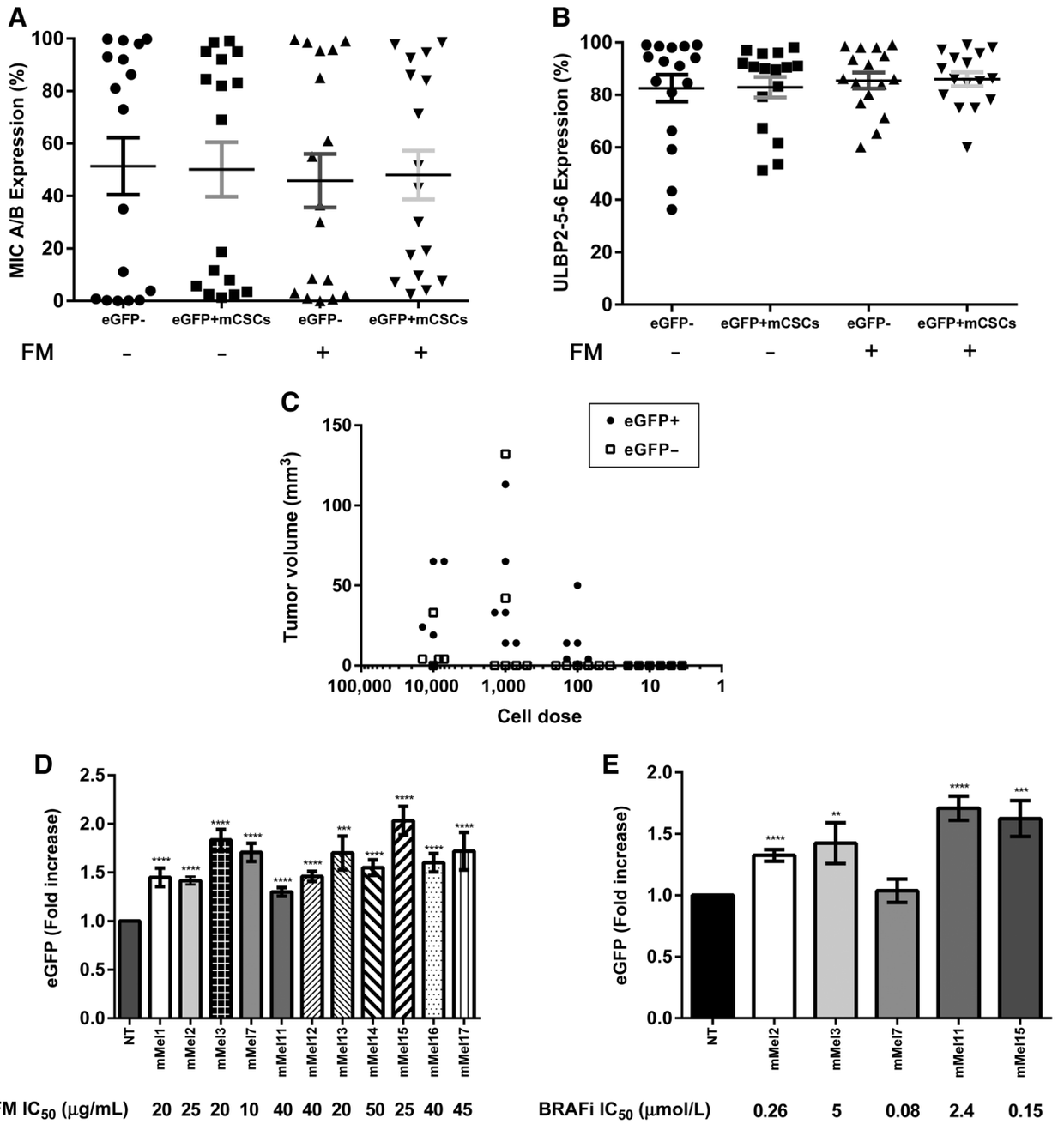

Figure 1.

Putative mCSCs express ligands for CIK cells, are tumorigenic, and relatively resistant to CHT. Putative mCSCs were visualized as eGFP$^+$ following lentiviral transduction with the lentiviral CSC-detector (LV.Oct4.eGFP). **A** and **B,** Mean (±SEM) membrane expression of MIC A/B ($n = 17$) and ULBP2-5-6 ($n = 16$) were comparable between eGFP$^+$ mCSCs and eGFP$^-$ melanoma cells before and after *in vitro* treatment with fotemustine (FM). MIC A/B expression in eGFP$^+$ mCSCs and eGFP$^-$ cells before (50.1% ± 10.4% and 51.4 ± 10.9, respectively) and after fotemustine treatment (48.0% ± 9.3% and 45.8 ± 10.2, respectively). **B,** ULBP2-5-6 expression in eGFP$^+$ mCSCs and eGFP$^-$ cells before (82.6% ± 5% and 82.9 ± 4, respectively) and after fotemustine treatment (85.5% ± 3% and 86 ± 3, respectively). **C,** Tumorigenic cell frequency evaluation by LDA. Summary of tumor volume (*y*-axis) in mice subcutaneously inoculated with decreasing doses of eGFP$^+$ or eGFP$^-$ melanoma cells (*x*-axis) in LDAs as described in Materials and Methods. Each symbol represents a mouse. Tumorigenic cell frequency in eGFP$^+$ fraction was 1:42 (lower frequency: 1 in 103; upper frequency: 1 in 17; X^2 (Pearson): 2,226; *P* value: 0,5269); tumorigenic cell frequency in eGFP$^-$ fraction was 1:4,870 (lower frequency: 1 in 12.467; upper frequency: 1 in 1.902; X^2 (Pearson): 1,233; *P* value: 0,7452). Viable eGFP$^+$ mCSCs enrichment after CHT (**D**) or targeted therapy (**E**). LV.Oct4.eGFP–transduced melanoma cells were treated with the IC_{50} dose of fotemustine or BRAFi for 72 hours. The eGFP enrichment for each melanoma culture ($n = 11$; $n = 5$), expressed as fold increase, was calculated for each experiment separately to compare fotemustine- or BRAFi-treated samples with their internal untreated control. In all cases, viable eGFP$^+$ cells were significantly enriched after CHT ($P \leq 0.0004$) and after BRAFi ($P \leq 0.0018$ except for mMel7, $P = 0.6781$).

Published OnlineFirst November 4, 2016; DOI: 10.1158/1078-0432.CCR-16-1524

Table 2. Immunophenotype of melanoma cell cultures: stemness markers

n. Melanoma	OCT4[a]	SOX-2[a]	NANOG[a]	ALDH high[b]	MITF[minus,a]	ABCG2[b]
mMel1	11	16	22	9	16	12
mMel2	14	22	3	9	17	12
mMel3	15	18	11	29	17	12
mMel7	22	19	16	9	10	3
mMel11	9	14	18	10	6	2
mMel12	18	18	15	11	11	8
mMel13	15	21	9	10	15	6
mMel14	14	29	12	6	6	2
mMel15	9	0	7	6	8	1
mMel16	19	20	8	7	58	2
mMel17	11	20	7	9	12	7
Average	14	18	12	10	16	6
SEM	1	2	2	2	4	1

[a]Value is expressed as percentage of positive cells.
[b]Value is expressed as percentage of viable positive cells.

(data not shown). Also the expression of programmed death-ligand 1 (PD-L1) was negligible (Table 1).

Additional molecules reported in the literature as mCSC phenotype–associated were also evaluated. OCT4, NANOG, SOX2, ATP Binding Cassette G2 (ABCG2), and aldehyde dehydrogenase (ALDH) were each detected in all samples at expressions averaging 14% ± 1.3%, 12% ± 1.7%, 18% ± 2.1%, 6% ± 1.3%, and 10% ± 1.9%, respectively (Table 2). Melanoma cells negative for MITF expression averaged 16% ± 4.4% (Table 2).

Tumorigenicity of putative mCSCs. To assess the tumorigenic potential of putative eGFP$^+$ mCSCs, we subcutaneously transplanted NOD/SCID mice with scalar dilutions (from 10 to 1 × 10^4) of eGFP$^+$ and eGFP$^-$ melanoma cells separated by FACS. Nine weeks after transplant, palpable tumors were evident in 4 of 6 mice injected with the highest dose of eGFP$^+$ cells compared with 1 of 6 in mice transplanted with the corresponding eGFP$^-$ cell dose. Limiting dilution analysis performed with L-Calc software indicated that the average frequency of tumorigenic melanoma cells, 12 weeks posttransplant, was 1/42 for eGFP$^+$ melanoma cells and 1/4,870 for eGFP$^-$ melanoma cells (Fig. 1C).

Sensitivity of putative mCSCs to CHT or molecular targeted therapy in vitro. We explored putative mCSC sensitivity to CHT treatment. Each of the 11 melanoma cell cultures was treated *in vitro* for 72 hours with a culture-specific dose (IC_{50}) of fotemustine to attain a 50% melanoma kill. Fotemustine sensitivity differed among the melanomas, such that IC_{50} ranged between 10 and 50 μg/mL (Fig. 1D). Activity against mCSCs was calculated by the rate of eGFP positivity among viable cells at treatment end. The rate of viable eGFP$^+$ mCSCs significantly increased after CHT (mean fold increase 1.61 ± 0.04) as compared with the untreated controls ($n = 62$ $P < 0.0001$), which confirmed their reduced sensitivity to conventional CHT (Fig. 1D). Comparable results were obtained treating *braf*-mutated melanomas ($n = 5$) with BRAFi dabrafenib (culture-specific IC_{50} dose, ranging between 0.08 and 5 μmol/L). Even in this case, the reduced sensitivity of mCSCs was assumed by their increased rate (1.5 ± 0.11 fold, $n = 20$ $P < 0.0001$) following treatment with BRAFi dabrafenib (Fig. 1E).

Immunotherapy with CIK cells against mCSC that survived chemo- or targeted therapy *in vitro*

Generation of CIK cells from patients. CIK cell activity against the mCSCs that survived fotemustine or BRAFi was assessed *in vitro*. CIK cells were generate from 8 of our 11 patients (described above), as PBMCs were unavailable for three patients in the study cohort. Within 3 to 4 weeks, cells from fresh or cryopreserved PBMCs were successfully expanded *ex vivo*, per a standard protocol with timed additions of IFNγ, Ab-anti-CD3, and IL2 (29–32). The median expansion of CIK cells was 29-fold (range 16- to 125-fold).

The mature CIK cell subset coexpressing CD3 and CD56 molecules (CD3$^+$CD56$^+$) was detected at a rate of 39% (range: 25%–58%), and 77% (69%–89%) of CD3$^+$ cells concurrently expressed CD8$^+$ (Supplementary Fig. S2A). Our results were comparable with previously published data (28, 29).

Pure natural killer (CD3$^-$CD56$^+$) cell presence was negligible (<5%, data not shown). The median membrane expression of NKG2D and DNAM-1 receptors was 84% (range: 69%–89%) and 97% (range: 89%–100%), respectively (Supplementary Fig. S2A).

In vitro killing of mCSCs surviving chemo- or targeted therapy by CIK cells. CIK cells efficiently killed melanoma cells that survived CHT and were enriched in putative eGFP$^+$ mCSCs *in vitro*. Mean tumor-specific killing values were determined at decreasing E:T ratios. They resulted as 95% ± 2% (40/1), 85% ± 3% (20/1), 68% ± 4% (10/1), 54% ± 4% (5/1), 40% ± 4% (3:1), 29% ± 5% (1:1), 22% ± 4% (1/2), and 19% ± 3% (1/3), which agreed with results obtained against untreated controls (Fig. 2A).

CIK cells were autologous-matched to melanoma targets in 8 of 11 cases; the three remaining melanomas were targeted with CIK cells from allogeneic patients only.

Comparable results were obtained when CIK cells were challenged against melanoma cells that survived BRAFi dabrafenib (Fig. 2C).

Our findings confirmed that the killing activity of CIK cells involved eGFP$^+$ mCSCs. Immunotherapy killing by CIK cells resulted in no relative increase of eGFP$^+$ mCSCs in the viable cell population ($P = 0.87$); instead, they were enriched after treatments with chemo- or targeted therapy of the same melanoma ($P < 0.0001$). The activity of CIK cells against eGFP$^+$ mCSCs is summarized in Fig. 2B and D.

In selected experiments ($n = 5$), we confirmed that the expression levels of NKG2D ligands (MIC A/B, ULBP2-5-6) and PDL-1 were comparable in eGFP$^+$ mCSCs before and after treatments (Supplementary Fig. S3A–S3C).

Published OnlineFirst November 4, 2016; DOI: 10.1158/1078-0432.CCR-16-1524

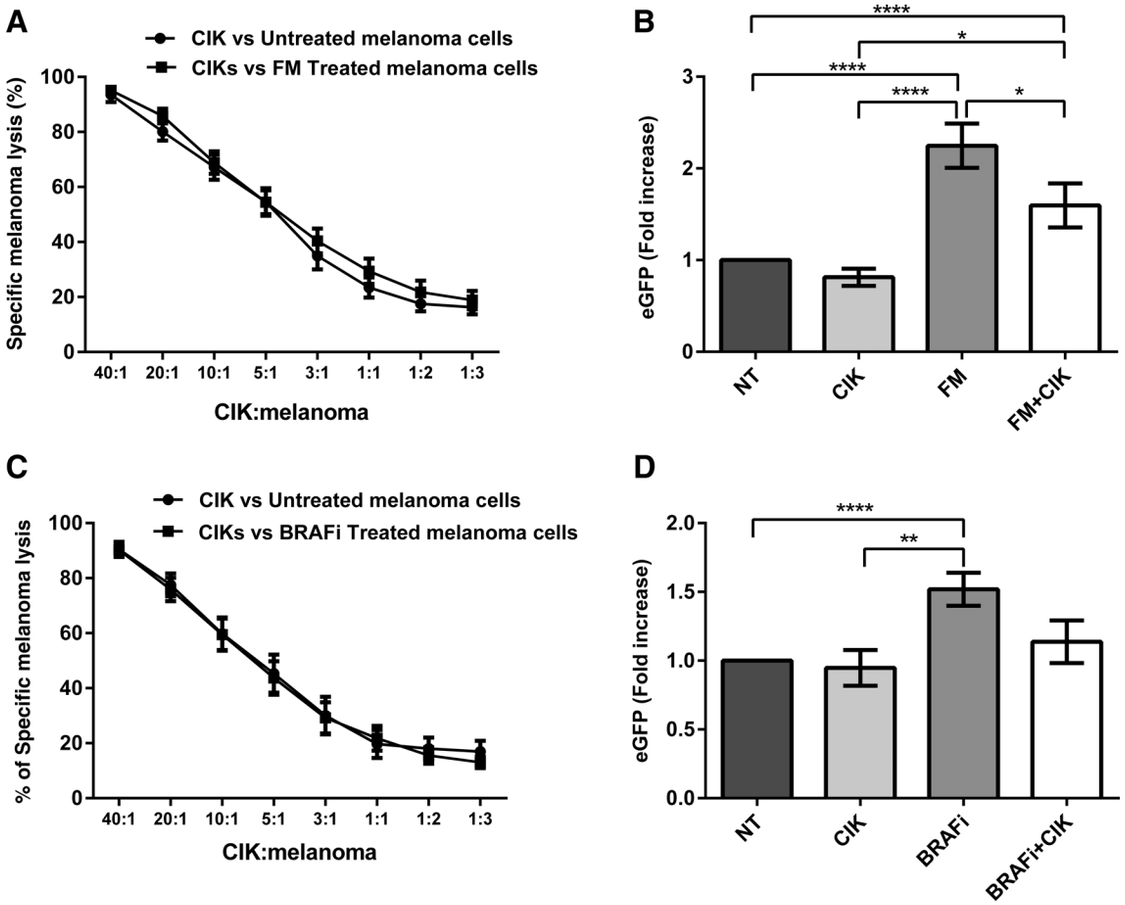

Figure 2.

Killing activity of chemo- or targeted therapy surviving mCSCs by patient-derived CIK cells. **A** and **C,** Patient-derived CIK cells efficiently killed *in vitro* melanoma targets that survived 72-hour treatment with fotemustine (FM+CIK; $n = 11$) or with dabrafenib (BRAFi+CIK; $n = 5$); results were comparable with those observed in melanomas treated with CIK immunotherapy alone. Tumor killing was performed after coculturing mature CIK cells with melanoma targets for 72 hours to and evaluated by both flow cytometry assay and by CellTiter-Glo Luminescent Cell Viability Assay. Mean values of tumor-specific killing are reported at decreasing CIK:Melanoma ratios. **B** and **D,** The activity against mCSCs was explored by tracking the rate of viable eGFP$^+$ mCSCs among surviving melanoma targets at the IC_{50} (E:T between 10:1 and 2:1) point of the killing curve. eGFP$^+$ mCSCs were spared by CHT ($n = 11$) or targeted therapy ($n = 5$), but efficiently killed by patient-derived CIK cells.

We compared the killing ability of autologous CIK cells with that of allogenic CIK cells against identical melanoma targets. The killing curves of autologous and allogeneic CIK cells trended similarly; the specific values for melanoma killing by autologous and allogenic CIK cells are reported in Supplementary Fig. S2B.

Immunotherapy activity of CIK cells against mCSCs in vivo. To verify that putative mCSCs can survive CHT, yet retain sensitivity to immunotherapy with CIK cells, we replicated our *in vitro* findings *in vivo*. The experiments utilized NOD/SCID mice bearing tumors generated by subcutaneously implanted LV.Oct4.eGFP–engineered melanoma cells from two different patients (mMel7 and mMel11). We explored the activity of CHT and immunotherapy with CIK cells, alone and in sequence.

The experimental design is detailed in Fig. 3A.

For group A, infusion of autologous CIK cells for two weeks ($n = 6$; 1×10^7 every 4 days) and CHT ($n = 6$; 600 μg/mouse, days 1;15) yielded significant tumor (mMel11) response, indicated by significant decrease of Ki67 proliferation index ($P < 0.0001$, Fig. 3B).

CHT spared eGFP$^+$ mCSCs that were instead killed by immunotherapy. The rate of residual viable eGFP$^+$mCSCs, compared to untreated controls ($n = 6$) was in fact significantly increased by fotemustine ($P = 0.0005$) but not by CIK cells ($P = 0.3250$, Fig. 3C).

Similar results were obtained with the intravenous infusion of allogenic CIK cells for two weeks (1×10^7 every 5 days; mMel7; Supplementary Fig. S4A and S4B).

In addition, we assessed the effect of sequential treatment with CHT and immunotherapy (group B, Fig. 3A). In two separate experiments, CIK cells were infused intravenously (1×10^7 every 4 days) following initial treatment with fotemustine (600 μg, day 1;15). Our results indicated that CIK cells ($n = 12$) not only retained significant antitumor activity ($P < 0.0001$), but that they also involved putative eGFP$^+$ mCSCs. The rate of viable eGFP$^+$ mCSCs assessed in residual tumors explanted at the end of the experiments was comparable with untreated controls ($n = 10$); on the contrary, a significant increment was observed and also maintained over time in mice treated with CHT alone ($n = 12$, $P < 0.05$; Fig. 3D and E; Supplementary Fig. S4C and S4D).

Published OnlineFirst November 4, 2016; DOI: 10.1158/1078-0432.CCR-16-1524

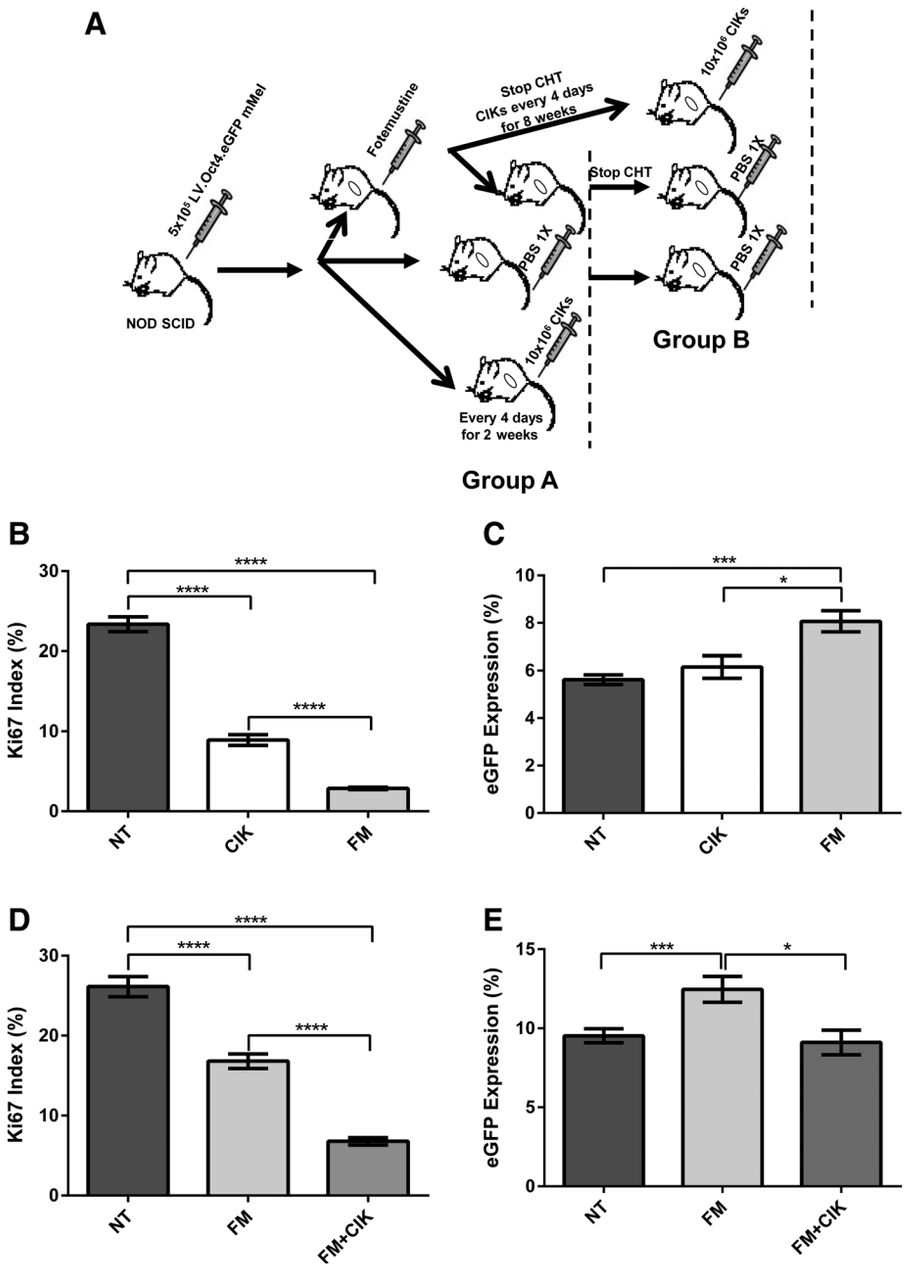

Figure 3.

In vivo activity of CIK cells against autologous mCSCs. **A,** Experimental design: NOD/SCID mice ($n = 40$) were subcutaneously inoculated with melanoma cells (from patient mMel 11) engineered with the CSC-detector (LV. Oct4.eGFP). Mice with palpable tumors were divided into three treatment cohorts. CIK-immunotherapy cohort ($n = 12$) received 4 intravenous infusions, each with 1×10^7 autologous mature CIK cells, CHT cohort ($n = 18$) was treated with 2 intraperitoneal injections (days 1;15) of fotemustine (600 μg/mouse). Mice injected ($n = 10$) with PBS alone were used as the untreated control. **B,** An early part of the experiment (Group A) was terminated and tumors analyzed at day +15; both CHT ($n = 6$) and CIK cells ($n = 6$) exerted significant antitumor activity, assessed by reduction of tumor Ki67 proliferative index compared with the controls ($n = 6$; $P < 0.0001$). **C,** The rate of residual viable eGFP$^+$ mCSCs was significantly increased by CHT ($P = 0.0005$) but not by immunotherapy with CIK cells. **D,** A second branch of the experiment (Group B) proceeded beyond day +15 to explore the effect of the chemo-immunotherapy combination. Mice ($n = 6$) from initial CHT cohort (treated with fotemustine on days 1;15) started intravenous infusions with CIK cells. Remaining mice from all initial cohorts [CIK-immunotherapy ($n = 6$), CHT ($n = 6$), and PBS cohorts ($n = 4$)] acted as controls and continued to be infused with PBS alone. The sequential chemo-immunotherapy treatment resulted in significant antitumor activity (reduction of tumor Ki67 proliferative index compared with untreated controls) ($P < 0.0001$). **E,** Activity against mCSCs was indirectly assumed as the rate of residual viable eGFP$^+$mCSCs, after sequential chemo-immunotherapy, was significantly decreased compared to mice treated with fotemustine only ($P = 0.0229$). All the results were expressed as mean ± SEM and analyzed by the unpaired *t* test.

The ability of CIK cells to localize and infiltrate tumor sites was confirmed by IHC detection of CD3$^+$ cells (Supplementary Fig. S5A–S5C).

Finally, CIK cell activity against putative mCSCs was confirmed in PDX models that were generated by direct subcutaneous implantation of fresh tumor samples from two patients in NOD/SCID mice (see Fig. 4A and Materials and Methods). Autologous CIK cell infusion for eight weeks (1×10^7 every 7 days) exerted significant antitumor activity ($n = 14$) as compared with untreated controls ($n = 13$; Fig. 4B). The antitumor activity was shown to also involve putative mCSCs, as evidenced by no observed significant enrichment of viable eGFP$^+$ mCSCs in residual tumors ($P = 0.3$; Fig. 4C).

Discussion

This work represents the first report of the immunotherapy activity with CIK cells against autologous chemo-surviving mCSCs *in vitro* and *in vivo*.

Previously, we provided proof of concept that CIK cells could kill autologous melanoma *in vitro*, including a subset of cells with stemness features (31, 32). Here, we build on those findings and demonstrate that putative mCSCs are, indeed, relatively resistant

Published OnlineFirst November 4, 2016; DOI: 10.1158/1078-0432.CCR-16-1524

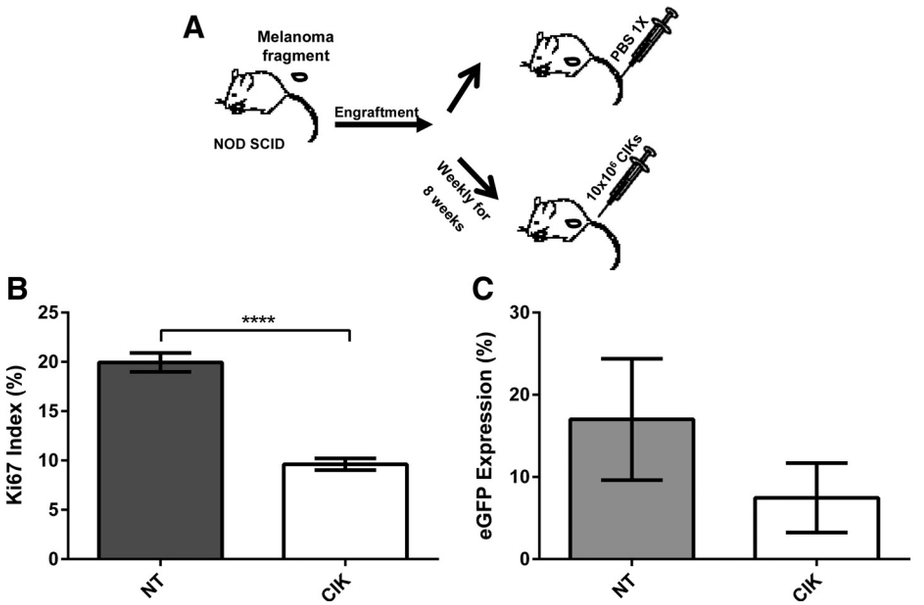

Figure 4.

In vivo activity of autologous CIK cells in PDX models. **A,** Experimental design: NOD/SCID mice were subcutaneously implanted with a tumor fragment (8 mm^3) from patient-derived melanoma biopsy (mMel2, $n = 20$; mMel3 $n = 7$). **B,** Intravenous immunotherapy treatment (10^7 CIK cells/mouse, weekly for 8 total infusions) started 1 week after tumor implantation ($n = 14$) and resulted in significant antitumor activity (assessed by Ki67 tumor proliferative index) compared with controls ($P < 0.0001$). **C,** Activity against mCSCs was indirectly assumed as the rate of residual viable $eGFP^+$ mCSCs after immunotherapy treatment, assessed in explanted tumors at experiment end, was comparable with untreated controls ($P = 0.3071$). All the results were expressed by mean ± SEM and analyzed by the unpaired *t* test.

to conventional CHT, yet sensitive to MHC-independent immune attack by autologous CIK cells. Furthermore, our observations *in vivo* confirmed the activity potential of CIK cells against mCSCs in a sequential treatment strategy. In selected cases of melanoma harboring *braf* mutations, we confirmed a similar effect *in vitro* with BRAFi dabrafenib than CHT. The ability to target mCSCs gives new rationale for considering CIK cells among adoptive immunotherapy approaches against melanoma. Currently, checkpoint inhibitors dominate center stage in melanoma immunotherapy. However, adoptive immunotherapy may also have an important role for prospective applications in dedicated settings, such as for the proportion of patients who fail to respond to upfront treatment with either anti-CTLA4 or anti-PD1 antibodies, or who experience relapses after initial response (51, 52). Similar scenarios may include relapses following molecular targeted therapy in patients with *braf*-mutated melanoma.

Expansion and reinfusion of tumor-infiltrating lymphocytes (TIL) or genetically redirected T cells have already demonstrated great potential and provided proof of clinical activity (53). Their activity induces or forces an adaptive immune response targeting precise HLA-restricted tumor-associated antigens (TAA). CIK cells represent an alternate approach that exploits the killing mechanisms of the innate immune system (e.g., natural killer cells or γδ T lymphocytes). Such an approach may be advantageous against infrequent mechanisms of melanoma immune escape, such as abnormalities or downregulation of HLA molecules that impair strategies based on TAA-specific lymphocytes or the effector phase of checkpoint inhibitors. Furthermore, such tumor defense mechanisms may be more pronounced in quiescent mCSCs that might not share or properly present TAAs (54). Treatment with CIK cells might be offered to virtually all patients, without restriction based on HLA haplotype. Clinical application of adoptive immunotherapy, however, is highly limited by logistic issues regarding cell preparation and production costs balanced against safe manufacturing procedures (GMP). The intense *ex vivo* expansibility of CIK cells and their cost-effectiveness can be shown to compare favorably with other approaches based on TAA-specific or genetically redirected lymphocytes. On the basis of our data, we tried to calculate the theoretical dose of CIK cells (per kg) each patient would have received. If we assume 50 mL of peripheral blood (day 0) is collected initially, then the final average cumulative dose of mature CIK cells per patient would have been clinical relevant (2.3×10^8 CIK cells/kg, SEM ± 0.53).

Support for the possibility of positive synergism between adoptive immunotherapy and checkpoint inhibitor antibodies in melanoma comes from preclinical evidence (55) that may also have a rationale with CIK cells. Patients would double-benefit from the MHC-unrestricted approach plus stimulation of antitumor adaptive immune response. CIK cells, as T-activated lymphocytes, do express PD-1 molecules but the functional role and potential benefit of modulation with checkpoint inhibitors remains undefined, despite its suggestion in selected settings (56).

CHT for the treatment of metastatic melanoma is less common due to the availability of more effective therapeutic approaches. Nevertheless, CHT may still be considered for patients relapsing after immunotherapy or molecular targeted treatments. In our model, the point of using fotemustine was to functionally characterize and define the "clinical relevance" of putative mCSCs that might survive such treatment. Furthermore, we found consistent results even in the case of *braf*-mutated melanoma treated *in vitro* with BRAFi. Our findings support the concept that mCSCs may be, at least partially, resistant also to molecular targeted approaches. On these bases, there may be rationale to explore synergisms with immunotherapy strategies that demonstrated activity against mCSCs.

In recent years, various CSC markers have been reported in several cancer types; however, no conclusive consensus exists. Our strategy was designed specifically to visualize a subset of melanoma cells capable of activating *oct4*, the main stem-related gene endowed with peculiar intrinsic biologic features. CSCs can be defined by their relative dormancy or by their ability to form spheres or to initiate tumors *in vivo*. Our previous study showed that putative $eGFP^+$ mCSCs displayed a slow-growing phenotype compared with their $eGFP^-$ counterparts, and we demonstrated that only putative $eGFP^+$ mCSCs were able to generate spheroids

Published OnlineFirst November 4, 2016; DOI: 10.1158/1078-0432.CCR-16-1524

(31). However, for conclusive evidence, the reliability of any CSC marker, even OCT4, should be tested experimentally via the *in vivo* tumor-initiating assay that is currently considered the most reliable standard test for CSC analysis. In the current study, we demonstrated that eGFP$^+$ mCSCs possess higher tumorigenic potential *in vivo* compared with their eGFP$^-$ counterparts, resulting in potentially enriched cells endowed with stemness features.

We are aware that our system may have limits and cannot ensure that all mCSCs are detected. Nevertheless, we aimed to demonstrate that the eGFP$^+$ mCSCs, even if not all of them are visualized, may survive conventional treatments but are killed by CIK cells.

Such a melanoma cell subset is less sensitive to conventional CHT compared with other melanoma cells, at least enough to be considered a relevant target from a clinical perspective.

We set up two distinct *in vivo* models, the first with melanoma cell cultures and the second with PDX. We observed consistent findings of chemo- and immune-sensitivity in mCSCs. When working with patient-derived samples, the possibility for experimental replicates is limited. Nevertheless, the results obtained in all our models were consistent with *in vitro* findings. We acknowledge that our experimental design and related endpoints were conceived to assess the effect of treatments on mCSCs. Even with these considerations, mice treated with sequential chemo-immunotherapy showed a trend of improved survival compared with controls (Supplementary Fig. S6). Overall the therapeutic meaningfulness of our findings may be indirectly derived by the clinical relevance attributed to CSCs.

Our work demonstrates that immunotherapy with CIK cells is active against a "relevant" target like melanoma cells surviving chemo or molecular targeted therapy and enriched in mCSCs. Adoptive immunotherapy approaches with CIK cells could be developed and integrated with ongoing treatment strategies for selected subsets of melanoma patients.

Disclosure of Potential Conflicts of Interest

G. Grignani reports receiving other commercial research support from Bayer, Lilly, Novartis, Pfizer, and PharmaMar and is a consultant/advisory board member for Bayer, Lilly, Novartis, and PharmaMar. No potential conflicts of interest were disclosed by the other authors.

Authors' Contributions

Conception and design: D. Sangiolo, L. Gammaitoni, F. Carnevale-Schianca, M. Aglietta

Development of methodology: D. Sangiolo, L. Gammaitoni

Acquisition of data (provided animals, acquired and managed patients, provided facilities, etc.): L. Giraudo, M. Macagno, V. Leuci, G. Mesiano, R. Rotolo, A. Zaccagna, A. Pisacane, R. Senetta, M. Cangemi, G. Cattaneo, V. Martin, V. Coha, S. Gallo, Y. Pignochino, A. Sapino, G. Grignani, F. Carnevale-Schianca

Analysis and interpretation of data (e.g., statistical analysis, biostatistics, computational analysis): D. Sangiolo, L. Gammaitoni, L. Giraudo, M. Macagno, V. Leuci, G. Mesiano, R. Rotolo, F. Sassi, M. Sanlorenzo, R. Senetta, M. Cangemi, G. Cattaneo, V. Martin, Y. Pignochino, G. Grignani, M. Aglietta

Writing, review, and/or revision of the manuscript: D. Sangiolo, L. Gammaitoni, L. Giraudo, M. Macagno, V. Leuci, G. Mesiano, R. Rotolo, M. Sanlorenzo, M. Cangemi, G. Cattaneo, V. Martin, Y. Pignochino, G. Grignani, F. Carnevale-Schianca, M. Aglietta

Administrative, technical, or material support (i.e., reporting or organizing data, constructing databases): V. Coha

Study supervision: D. Sangiolo, G. Grignani, M. Aglietta

Acknowledgments

The phOCT4.EGFP1 vector was a kind gift from Dr. W. Cui (IRDB, Imperial College London). We are grateful to Dr. E. Vigna (University of Torino, Candiolo Cancer Institute, FPO-IRCCS, Candiolo, Turin, Italy) who provided the transfer vector pRRL.sin.PPT.hPGK.EGFP.Wpre (LV-PGK.EGFP). The authors sincerely thank Joan Leonard (Leonard Editorial Services, LLC) for the linguistic revision and editorial assistance. The authors also thank P. Bernabei for sorting services.

Grant Support

This study was financed in part by the "Associazione Italiana Ricerca sul Cancro" (AIRC) MFAG 2014 N.15731; IG grant N.11515, FPRC ONLUS 5 × 1000, Ministero della Salute 2012; Ricerca Finalizzata-Giovani Ricercatori Ministero della Salute (GR-2011-02349197), University of Torino Fondo Ricerca Locale 2013. L. Giraudo was sponsored by the 'Associazione Italiana Ricerca sul Cancro–AIRC'; M. Macagno was sponsored by Ricerca Finalizzata-Giovani Ricercatori Ministero della Salute; V. Leuci and Y. Pignochino received a fellowship by MIUR (University of Turin); M. Sanlorenzo received support from L'Oréal-UNESCO For Women in Science Fellowship 2016.

The costs of publication of this article were defrayed in part by the payment of page charges. This article must therefore be hereby marked *advertisement* in accordance with 18 U.S.C. Section 1734 solely to indicate this fact.

Received June 21, 2016; revised October 13, 2016; accepted October 20, 2016; published OnlineFirst November 4, 2016.

References

1. National Collaborating Centre for Cancer (UK). Melanoma: assessment and management. London, United Kingdom: National Institute for Health and Care Excellence (UK); 2015.
2. McArthur GA, Chapman PB, Robert C, Larkin J, Haanen JB, Dummer R, et al. Safety and efficacy of vemurafenib in BRAF(V600E) and BRAF (V600K) mutation-positive melanoma (BRIM-3): extended follow-up of a phase 3, randomised, open-label study. Lancet Oncol 2014;15:323–32.
3. Hauschild A, Grob JJ, Demidov LV, Jouary T, Gutzmer R, Millward M, et al. Dabrafenib in BRAF-mutated metastatic melanoma: a multicentre, open-label, phase 3 randomised controlled trial. Lancet 2012; 380:358–65.
4. Flaherty KT, Robert C, Hersey P, Nathan P, Garbe C, Milhem M, et al. Improved survival with MEK inhibition in BRAF-mutated melanoma. N Engl J Med 2012;367:107–14.
5. Hodi FS, O'Day SJ, McDermott DF, Weber RW, Sosman JA, Haanen JB, et al. Improved survival with ipilimumab in patients with metastatic melanoma. N Engl J Med 2010;363:711–23.
6. Weber JS, D'Angelo SP, Minor D, Hodi FS, Gutzmer R, Neyns B, et al. Nivolumab versus chemotherapy in patients with advanced melanoma who progressed after anti-CTLA-4 treatment (CheckMate 037): a randomised, controlled, open-label, phase 3 trial. Lancet Oncol 2015;16: 375–84.
7. Larkin J, Hodi FS, Wolchok JD. Combined nivolumab and ipilimumab or monotherapy in untreated melanoma. N Engl J Med 2015;373:1270–1.
8. Watson I, Dominguez PP, Donegan E, Charles Z, Robertson J, Adam EJ. NICE guidance on pembrolizumab for advanced melanoma. Lancet Oncol 2016;17:21–2.
9. Hall CJ, Doss S, Robertson J, Adam J. NICE guidance on ipilimumab for treating previously untreated advanced (unresectable or metastatic) melanoma. Lancet Oncol 2014;15:1056–7.
10. Coit DG, Thompson JA, Algazi A, Andtbacka R, Bichakjian CK, Carson WE, et al. Melanoma, version 2.2016, NCCN clinical practice guidelines in oncology. J Natl Compr Canc Netw 2016;14:450–73.
11. Dummer R, Schadendorf D, Ascierto PA, Larkin J, Lebbé C, Hauschild A. Integrating first-line treatment options into clinical practice: what's new in advanced melanoma? Melanoma Res 2015;25:461–9.
12. Robbins PF, Kassim SH, Tran TL, Crystal JS, Morgan RA, Feldman SA, et al. A pilot trial using lymphocytes genetically engineered with an NY-ESO-1-

reactive T-cell receptor: long-term follow-up and correlates with response. Clin Cancer Res 2015;21:1019–27.
13. Robbins PF, Morgan RA, Feldman SA, Yang JC, Sherry RM, Dudley ME, et al. Tumor regression in patients with metastatic synovial cell sarcoma and melanoma using genetically engineered lymphocytes reactive with NY-ESO-1. J Clin Oncol 2011;29:917–24.
14. Clarke MF, Dick JE, Dirks PB, Eaves CJ, Jamieson CH, Jones DL, et al. Cancer stem cells–perspectives on current status and future directions: AACR Workshop on cancer stem cells. Cancer Res 2006;66:9339–44.
15. Croker AK, Allan AL. Cancer stem cells: implications for the progression and treatment of metastatic disease. J Cell Mol Med 2008;12:374–90.
16. Islam F, Gopalan V, Smith RA, Lam AK. Translational potential of cancer stem cells: A review of the detection of cancer stem cells and their roles in cancer recurrence and cancer treatment. Exp Cell Res 2015;335:135–47.
17. Colak S, Medema JP. Cancer stem cells–important players in tumor therapy resistance. FEBS J 2014;281:4779–91.
18. Cojoc M, Mäbert K, Muders MH, Dubrovska A. A role for cancer stem cells in therapy resistance: cellular and molecular mechanisms. Semin Cancer Biol 2015;31:16–27.
19. Ciurea ME, Georgescu AM, Purcaru SO, Artene SA, Emami GH, Boldeanu MV, et al. Cancer stem cells: biological functions and therapeutically targeting. Int J Mol Sci 2014;15:8169–85.
20. Rycaj K, Tang DG. Cancer stem cells and radioresistance. Int J Radiat Biol 2014;90:615–21.
21. Kaiser J. The cancer stem cell gamble. Science 2015;347:226–9.
22. Gammaitoni L, Leuci V, Mesiano G, Giraudo L, Todorovic M, Carnevale-Schianca F, et al. Immunotherapy of cancer stem cells in solid tumors: initial findings and future prospective. Expert Opin Biol Ther 2014;14:1259–70.
23. Li Y, Rogoff HA, Keates S, Gao Y, Murikipudi S, Mikule K, et al. Suppression of cancer relapse and metastasis by inhibiting cancer stemness. Proc Natl Acad Sci U S A 2015;112:1839–44.
24. Stuckey DW, Shah K. TRAIL on trial: preclinical advances in cancer therapy. Trends Mol Med 2013;19:685–94.
25. Vik-Mo EO, Nyakas M, Mikkelsen BV, Moe MC, Due-Tønnesen P, Suso EM, et al. Therapeutic vaccination against autologous cancer stem cells with mRNA-transfected dendritic cells in patients with glioblastoma. Cancer Immunol Immunother 2013;62:1499–509.
26. Cioffi M, Dorado J, Baeuerle PA, Heeschen C. EpCAM/CD3-Bispecific T-cell engaging antibody MT110 eliminates primary human pancreatic cancer stem cells. Clin Cancer Res 2012;18:465–74.
27. Visus C, Wang Y, Lozano-Leon A, Ferris RL, Silver S, Szczepanski MJ, et al. Targeting ALDH(bright) human carcinoma-initiating cells with ALDH1A1-specific $CD8^+$ T cells. Clin Cancer Res 2011;17:6174–84.
28. Sangiolo D, Martinuzzi E, Todorovic M, Vitaggio K, Vallario A, Jordaney N, et al. Alloreactivity and anti-tumor activity segregate within two distinct subsets of cytokine-induced killer (CIK) cells: implications for their infusion across major HLA barriers. Int Immunol 2008;20:841–8.
29. Todorovic M, Mesiano G, Gammaitoni L, Leuci V, Giraudo Diego L, Cammarata C, et al. Ex vivo allogeneic stimulation significantly improves expansion of cytokine-induced killer cells without increasing their alloreactivity across HLA barriers. J Immunother 2012;35:579–86.
30. Elia AR, Circosta P, Sangiolo D, Bonini C, Gammaitoni L, Mastaglio S, et al. Cytokine-induced killer cells engineered with exogenous T-cell receptors directed against melanoma antigens: enhanced efficacy of effector cells endowed with a double mechanism of tumor recognition. Hum Gene Ther 2015;26:220–31.
31. Gammaitoni L, Giraudo L, Leuci V, Todorovic M, Mesiano G, Picciotto F, et al. Effective activity of cytokine-induced killer cells against autologous metastatic melanoma including cells with stemness features. Clin Cancer Res 2013;19:4347–58.
32. Sangiolo D, Mesiano G, Gammaitoni L, Leuci V, Todorovic M, Giraudo L, et al. Cytokine-induced killer cells eradicate bone and soft-tissue sarcomas. Cancer Res 2014;74:119–29.
33. Lu PH, Negrin RS. A novel population of expanded human CD3+CD56+ cells derived from T cells with potent *invivo* antitumor activity in mice with severe combined immunodeficiency. J Immunol 1994;153:1687–96.
34. Schmidt-Wolf IG, Lefterova P, Johnston V, Huhn D, Blume KG, Negrin RS. Propagation of large numbers of T cells with natural killer cell markers. Br J Haematol 1994;87:453–8.
35. Baker J, Verneris MR, Ito M, Shizuru JA, Negrin RS. Expansion of cytolytic CD8(+) natural killer T cells with limited capacity for graft-versus-host disease induction due to interferon gamma production. Blood 2001;97:2923–31.
36. Verneris MR, Karami M, Baker J, Jayaswal A, Negrin RS. Role of NKG2D signaling in the cytotoxicity of activated and expanded CD8+ T cells. Blood 2004;103:3065–72.
37. Olioso P, Giancola R, Di Riti M, Contento A, Accorsi P, Iacone A. Immunotherapy with cytokine induced killer cells in solid and hematopoietic tumours: a pilot clinical trial. Hematol Oncol 2009;27:130–9.
38. Schmidt-Wolf IG, Finke S, Trojaneck B, Denkena A, Lefterova P, Schwella N, et al. Phase I clinical study applying autologous immunological effector cells transfected with the interleukin-2 gene in patients with metastatic renal cancer, colorectal cancer and lymphoma. Br J Cancer 1999;81:1009–16.
39. Verneris MR, Baker J, Edinger M, Negrin RS. Studies of ex vivo activated and expanded CD8+ NK-T cells in humans and mice. J Clin Immunol 2002;22:131–6.
40. Pizzitola I, Anjos-Afonso F, Rouault-Pierre K, Lassailly F, Tettamanti S, Spinelli O, et al. Chimeric antigen receptors against CD33/CD123 antigens efficiently target primary acute myeloid leukemia cells in vivo. Leukemia 2014;28:1596–605.
41. Tettamanti S, Marin V, Pizzitola I, Magnani CF, Giordano Attianese GM, Cribioli E, et al. Targeting of acute myeloid leukaemia by cytokine-induced killer cells redirected with a novel CD123-specific chimeric antigen receptor. Br J Haematol 2013;161:389–401.
42. Pizzitola I, Agostoni V, Cribioli E, Pule M, Rousseau R, Finney H, et al. In vitro comparison of three different chimeric receptor-modified effector T-cell populations for leukemia cell therapy. J Immunother 2011;34:469–79.
43. Rettinger E, Huenecke S, Bonig H, Merker M, Jarisch A, Soerensen J, et al. Interleukin-15-activated cytokine-induced killer cells may sustain remission in leukemia patients after allogeneic stem cell transplantation: feasibility, safety and first insights on efficacy. Haematologica 2016;101:e153–6.
44. Schmeel LC, Schmeel FC, Coch C, Schmidt-Wolf IG. Cytokine-induced killer (CIK) cells in cancer immunotherapy: report of the international registry on CIK cells (IRCC). J Cancer Res Clin Oncol 2015;141:839–49.
45. Todaro M, Meraviglia S, Caccamo N, Stassi G, Dieli F. Combining conventional chemotherapy and γδ T cell-based immunotherapy to target cancer-initiating cells. Oncoimmunology 2013;2:e25821.
46. Todaro M, Orlando V, Cicero G, Caccamo N, Meraviglia S, Stassi G, et al. Chemotherapy sensitizes colon cancer initiating cells to Vγ9Vδ2 T cell-mediated cytotoxicity. PLoS One 2013;8:e65145.
47. Dieli F, Stassi G, Todaro M, Meraviglia S, Caccamo N, Cordova A. Distribution, function and predictive value of tumor-infiltrating γδ T lymphocytes. Oncoimmunology 2013;2:e23434.
48. Gerrard L, Zhao D, Clark AJ, Cui W. Stably transfected human embryonic stem cell clones express OCT4-specific green fluorescent protein and maintain self-renewal and pluripotency. Stem Cells 2005;23:124–33.
49. Dull T, Zufferey R, Kelly M, Mandel RJ, Nguyen M, Trono D, et al. A third-generation lentivirus vector with a conditional packaging system. J Virol 1998;72:8463–71.
50. Zufferey R, Dull T, Mandel RJ, Bukovsky A, Quiroz D, Naldini L, et al. Self-inactivating lentivirus vector for safe and efficient in vivo gene delivery. J Virol 1998;72:9873–80.
51. Wolchok JD, Kluger H, Callahan MK, Postow MA, Rizvi NA, Lesokhin AM, et al. Nivolumab plus ipilimumab in advanced melanoma. N Engl J Med 2013;369:122–33.
52. Lee J, Kefford R, Carlino M. PD-1 and PD-L1 inhibitors in melanoma treatment: past success, present application and future challenges. Immunotherapy 2016;8:733–46.
53. Rosenberg SA, Yang JC, Sherry RM, Kammula US, Hughes MS, Phan GQ, et al. Durable complete responses in heavily pretreated patients with metastatic melanoma using T-cell transfer immunotherapy. Clin Cancer Res 2011;17:4550–7.

Published OnlineFirst November 4, 2016; DOI: 10.1158/1078-0432.CCR-16-1524

54. Sottile R, Pangigadde PN, Tan T, Anichini A, Sabbatino F, Trecroci F, et al. HLA class I downregulation is associated with enhanced NK-cell killing of melanoma cells with acquired drug resistance to BRAF inhibitors. Eur J Immunol 2016;46:409–19.
55. Gargett T, Yu W, Dotti G, Yvon ES, Christo SN, Hayball JD, et al. GD2-specific CAR T cells undergo potent activation and deletion following antigen encounter but can be protected from activation-induced cell death by PD-1 blockade. Mol Ther 2016;24:1135–49.
56. Poh SL, Linn YC. Immune checkpoint inhibitors enhance cytotoxicity of cytokine-induced killer cells against human myeloid leukaemic blasts. Cancer Immunol Immunother 2016;65:525–36.

Published OnlineFirst November 4, 2016; DOI: 10.1158/1078-0432.CCR-16-1524

Clinical Cancer Research

Cytokine-Induced Killer Cells Kill Chemo-surviving Melanoma Cancer Stem Cells

Loretta Gammaitoni, Lidia Giraudo, Marco Macagno, et al.

Clin Cancer Res 2017;23:2277-2288. Published OnlineFirst November 4, 2016.